

11:25:39

OCA PAD INITIATION - PROJECT HEADER INFORMATION

04/18/88

Active

Project #: E-25-M45  
Center #: R6474-OA0

Cost share #:  
Center shr #:

Rev #: 0  
OCA file #:  
Work type : RES  
Document : PO  
Contract entity: GTRC

Contract#: 19X-SB395C  
Prime #: DE-AC05-840R21400

Mod #:

Subprojects ? : N  
Main project #:

Project unit: ME Unit code: 02.010.126  
Project director(s):  
STACEY W M JR ME

Sponsor/division names: OAK RIDGE NAT'L LAB / MARTIN MARIETTA  
Sponsor/division codes: 240 / 001

Award period: 880118 to 880630 (performance) 880630 (reports)

Sponsor amount	New this change	Total to date
Contract value	20,000.00	20,000.00
Funded	20,000.00	20,000.00
Cost sharing amount		0.00

Does subcontracting plan apply ? : N

Title: ENGINEERING ASSISTANCE TO THE INTOR PROJECT

PROJECT ADMINISTRATION DATA

OCA contact: John B. Schonk

894-4820

Sponsor technical contact

Sponsor issuing office

TOM SHANNON  
(615)576-5500  
MARTIN MARIETTA ENERGY SYSTEMS  
P.O. BOX M  
OAK RIDGE, TN 37831

JOHN E. SCHULTZ  
(615)576-1448

SAME

Security class (U,C,S,TS) : U  
Defense priority rating : D0-E2  
Equipment title vests with: Sponsor

ONR resident rep. is ACO (Y/N): N  
GOVT supplemental sheet  
GIT

Administrative comments -

PROJECT INITIATION

ADMINISTERED UNDER THE USUAL MARTIN MARIETTA/OAK RIDGE T'S AND C'S.



## NOTICE OF PROJECT CLOSEOUT

Project No. E-25-M45

Center No. R6474-0A0

Project Director W. M. Stacey, Jr.

School/Lab ME

Sponsor Martin-Marietta Energy Systems, Inc./ Oak Ridge National Lab

Contract/Grant No. 19X-SB395C

GTRC XX GIT

Prime Contract No. DE-AC05-84OR21400

Title Engineering Assistance to the INTOR Project

Effective Completion Date 6/30/88 (Performance) 6/30/88 (Reports)

**Closeout Actions Required:**

None  
Final Invoice or Copy of Last Invoice -Already submitted  
X Final Report of Inventions and/or Subcontracts - Questionnaire sent to P/I.  
Government Property Inventory & Related Certificate - Already submitted  
Classified Material Certificate  
Release and Assignment - Already submitted  
Other

Includes Subproject No(s). \_\_\_\_\_

Subproject Under Main Project No. \_\_\_\_\_

Continues Project No. \_\_\_\_\_ Continued by Project No. \_\_\_\_\_

**Distribution:**

<u>X</u>	Project Director
<u>X</u>	Administrative Network
<u>X</u>	Accounting
<u>X</u>	Procurement/GTRI Supply Services
<u>X</u>	Research Property Management
<u>X</u>	Research Security Services

X Reports Coordinator (OCA)  
X GTRC  
X Project File  
X Contract Support Division (OCA)(2)  
 Other

## 1. CRITICAL ISSUES, INNOVATIONS & DATA BASE

### 1.1 Introduction

Three of the Critical Issues of Part 2 of Phase 2A of the INTOR Workshop were continued into this Phase because considerable progress was still expected from further work on them. These were impurity control, current drive and heating (with emphasis moving towards current drive) and electromagnetics. New topics were operational limits and confinement, and configuration and maintenance, the latter topic aiming at a critical comparison of different maintenance approaches. Blanket and first wall, the sixth topic among the Critical Issues was picked up again because it was expected that new information might lead to an up-dating of earlier conclusions.

During this Phase the INTOR Workshop was also charged with an analysis of proposed innovations to improve the Tokamak concept. A collection of proposals and a first analysis was made during an INTOR-related Specialists' Meeting. Those of the proposed innovations which looked promising and of sufficient impact were then picked up by the relevant INTOR groups for further treatment.

### 1.2 Impurity Control

During Part 3 of INTOR Phase 2A, work on impurity control has been directed towards: (a) updating previous assessments of experimental data for impurity control; (b) evaluating the potential for relevance INTOR of a number of innovative concepts; and (c) improving the consistency of plasma edge modelling, with particular emphasis upon model validation and improved prediction of divertor performance in INTOR-like tokamak reactors.

#### 1.2.1 Experimental Data

There has been a substantial amount of new data from both poloidal divertor and from limiter experiments in tokamaks. There is new further evidence that a divertor with an open geometry, of the type envisaged for INTOR, is capable of producing the high recycling conditions which are

necessary to minimize sputtering erosion of the divertor target. The concentration of impurities in the main plasma is generally lower for divertor experiments than for limiter experiments (except for the H-mode). However, the concentration of low-Z impurities (e.g. oxygen) are not affected as much as the level of high-Z impurities by a divertor. There is often substantial emission of radiation within the divertor region which is indicative of high recycling conditions. It appears that H-mode operation can be obtained most easily by operation with a poloidal divertor. In contrast, H-mode operation has been observed in only one limiter experiment. A detrimental aspect of the H-mode is that, in certain conditions, H-mode operation is accompanied by the accumulation of impurities on the plasma axis. Nonetheless, the temperature of the plasma in contact with the limiter during limiter operation is high. This is likely to lead to high rates of sputtering and erosion of the limiter. Experiments on TEXTOR indicate that exhaust of neutral gas can be quite efficiently performed by a pumped limiter.

#### 1.2.2 Innovative Impurity Control Schemes

Five innovative schemes for impurity control in INTOR have been considered: (i) flow reversal of impurities as a consequence of co-injection of neutral beams, (ii) formation of a stable radiative edge at the periphery of the plasma column; (iii) an ergodic edge layer; (iv) burial of helium in the divertor region, and (v) liquid divertor plates. The first three are not yet sufficiently well developed for them to be considered as candidates for the INTOR impurity control system. The last two show promise and further theoretical and experimental work, together with the appropriate design analyses, is strongly encouraged.

#### 1.2.3 Plasma Edge Modelling

Improvements have been made in the two dimensional numerical models used both for interpretation and prediction of plasma edge performance. Comparison of the edge conditions calculated using the models with conditions observed in experiments has enhanced confidence in such modelling. These models have been used to analyze the projected performance for the INTOR divertor.



As a consequence of this work, the conclusion is that a high recycling divertor with a tungsten target is the best available impurity control system to maintain a clean main plasma in INTOR and to ensure low target erosion during a fully inductive operational scenario. However, there are large uncertainties in plasma transport and in confinement requirements, and further research and development and continuous reassessment of the expected performance of the present INTOR impurity control system is needed. Impurity control with current drive during an ignited burn is potentially different due to the increased power loads. A stable radiating edge layer and, in this respect, flow reversal would be beneficial. During inductive ramp up, it is expected that adequate levels of high recycling can be established within the divertor. However, this is less certain in the case of non-inductive ramp up. Consideration has been given to the use, in INTOR-like conditions, of low-Z target material (e.g., carbon and beryllium). Such materials are unlikely to be suitable for the more extended technology phase unless the divertor target surface can be readily renewed.

Improved modelling of impurity transport indicates that the pumping requirements for exhaust of helium ash may be more demanding than those specified in Phase IIA (Parts 1 and 2), i.e.,  $\sim 2 \times 10^5 \ell/s$  of helium. Analysis of the innovative scheme for burial for helium in a continuously recoated metal layer within the divertor chamber indicates that it could be a useful adjunct to vacuum pumps.

Recent modelling confirms the previous prediction that divertor action provides efficient screening of the main plasma from impurities present in the edge. However, there remain many uncertainties (e.g., cross field transport of impurity ions sputtering by superthermal ions, etc.) and continuing experimental and theoretical studies are required.

An overall conclusion from Phase IIA (Part 3) is that the poloidal divertor will, for INTOR, offer many advantages over a pumped limiter. Nevertheless, certain aspects of impurity control are at present uncertain and both the conceptional design and the operational scenario for INTOR should be flexible in these particular respects.

### 1.3 Operational Limits and Confinement

Operational limits to stable tokamak operation, disruptions and the confinement properties of tokamak plasmas are key issues for INTOR. In these areas an updating of the data base has been undertaken and innovative ideas have been analyzed, in particular with respect to enhancing the beta limit. A specific effort was dedicated to advancing the ideal MHD stability analysis beyond the limits explored in the past.

#### 1.3.1 Beta Limit

Experimental results on the operational limit to the plasma beta correspond to values of the Troyon factor  $g$  in the range 3 to 3.5  $\% \cdot T_m/MA$ , provided that  $q_a$  is above a critical value which increases with decreasing  $A$ . A normal conductor TF coil set would be required to economically use such high beta values. For indented plasmas, while the ideal ballooning stability limit is enhanced, the kink mode is destabilized so that efficient wall stabilization is essential for achieving high beta. It remains uncertain whether this can be provided. The second stability regime of ideal ballooning modes can be reached either in D-shaped plasmas for sufficiently high  $q_0$  or in sufficiently indented plasmas. However, in these cases, kink mode instability is enhanced. Furthermore, a wide range of the plasma has to be nearly shear-free, a situation in which low- $n$  internal modes tend to be destabilized. Also resistive destabilization of high- $n$  modes is a concern. In conclusion, moderately elongated D-shapes ( $K \approx 2$ ) appear attractive for SIC INTOR and allow to enhance the plasma beta. Unconventional solutions to increase beta presently are too uncertain to rely upon at the present time.

#### 1.3.2. Density Limit

The density limit, if extrapolated according to common Murakami-Hugill-like scalings, tends to be a more stringent limitation to the plasma pressure, at temperatures  $T \leq 10$  keV, than the beta limit. However, the physics understanding of this limit is incomplete, and results for discharges with intense additional heating generally show an enhancement of the density limit and indicate large deviations from the Murakami-Hugill scaling. In JET, the density limit appears when the radiation losses become

equal to the power input, a criterion which, when extrapolated to INTOR, predicts an appreciably higher density limit than the Murakami-Hugill scaling. Quantitative predictions, however, sensitively depend on the plasma edge parameters in this case. The limit to the safety factor, at least at modest values of beta and for conventional circular and D-shaped plasmas, is greater than 2, 95% of the magnetic flux for poloidal divertor configurations. This limit is seen to increase to above 3 as the beta limit is approached or when the elongation is increased to beyond 2.

### 1.3.3 Disruptions

Operational limits are often due to the appearance of disruptions. The available data base on major disruptions was analyzed and the disruption specification for INTOR was updated. In view of results from JET and TFTR, very short energy quench times, of the order of 0.1 ms, must be considered to be a possibility in INTOR. The energy deposition profile in a poloidal divertor configuration remains unknown so that deposition of up to the total plasma kinetic energy on either the divertor plates or the first wall must be considered. The current quench rate is determined by the evolution of the plasma parameters after energy quench, taking account of the electromagnetic coupling to the surrounding passive conducting structures and the capacity of the active position control device. If efficient position control is provided for a maximum current decay rate of  $3 \times 10^8$  A/s appears appropriate for INTOR.

### 1.3.4 Confinement

Extrapolation of plasma confinement to INTOR still contains large uncertainties (by over one order of magnitude). Operating INTOR in a regime of improved confinement ("H-mode") is considered reasonable, although major uncertainties remain with respect to the reactor relevance of this regime. These uncertainties are related to the existence of controlled steady-state operation with low impurities, to its compatibility with RF heating and current drive, and to efficient power and particle exhaust under acceptable working conditions of the divertor plates and first wall. Also, the scaling of energy confinement in the H-mode remains uncertain, in particular with respect to plasma size, plasma temperature, heating power, and to some extent plasma current and density. These issues are key research items in the ongoing tokamak physics program and are expected to be clarified before the start of INTOR-like devices.

#### 1.4 Current Drive and Heating

A number of advances have recently transpired in understanding auxiliary heating and noninductive current generation (NCG). These theoretical and experimental achievements have confirmed the benefits of several new techniques and give the designers more latitude in conceiving a device with operational flexibility.

Respecting auxiliary heating, one particular accomplishment has been the testing of ion Bernstein wave heating (IBWH) on PLT [1]. A direct comparison with fast wave minority ( $\text{He}^3$ ) heating on PLT showed nearly identical results for heating efficiency,  $\bar{n}_e \Delta T_{i0}/P_{\text{rf}} = 6.7 \times 10^{19} \text{ KeV} \cdot \text{m}^{-3}/\text{MW}$ , with up to 650 kW of applied power. It is particularly noteworthy that IBWH results in very small ion tails, as the wave couples directly with the bulk ions. It is possible that this trait could result in favorable energy confinement for the ions, which remain nearly maxwellian. The launching structure for IBWH is attractive for a reactor; unlike a fast wave antenna, this launcher could be a pair of simple rectangular waveguides which, for frequencies about 130 MHz, would require a vertical opening of about one meter and horizontal width of  $\sim 2 \times 20 \text{ cm}$  through the first wall.

In contrast to IBWH, most other proposed auxiliary heating methods could also serve for NCG. The techniques most attractive for INTOR are neutral beam (NBCD), lower hybrid (LHCD), and fast wave (FWCD) current drive. These systems offer adequately high electric-to-driver power efficiency ( $\geq 50\%$ ) and acceptable cost levels such that they can be considered for bulk current drive at power levels approaching 100 MW. The theory of NCG has matured in recent years with the inclusion of realistic effects such as magnetic trapping, relativistic electron behavior, arbitrary ion charge, nonzero electric fields, Pfirsch-Schluter and bootstrap currents, and, for wave-driven currents, allowing for arbitrary wave polarizations, frequencies and phase speeds. Most importantly for INTOR, high power experiments with NCG are bearing out many of the theoretical predictions.

With regard to neutral beam injection, we note that NBCD on TFTR [2] has maintained a current of 1 MA at densities greater than  $1 \times 10^{19} \text{ m}^{-3}$  for 2 s with 6.0 MW of co-injection and 4.6 MW of counter-injection. Experimental evidence of NBCD has invariably been in good agreement with theoretical predictions, so we feel that NBCD would be a reliable option for high density



operation of INTOR. However, in order to achieve a centrally peaked current density profile it will be necessary to inject at energies  $\geq 1$  MeV. This is a difficult challenge which would require a period of negative ion source and accelerator development. Additionally, there is concern that such high beam energies may drive an Alfvén wave instability in the plasma, resulting in a possibly degraded NBCD efficiency.

At low densities the LHCD option appears to be complementary to the neutral beam. Experiments have shown impressive results at low densities: on JT-60 a current of 2 MA is maintained at  $\bar{n}_e = 3 \times 10^{18} \text{ m}^{-3}$  for 2.5 s with 3.0 MW of power [3]. The efficiency, defined as  $\gamma = \bar{n}_e I R / P [10^{20} \text{ A} \cdot \text{W}^{-1} \cdot \text{m}^{-2}]$ , is theoretically an increasing function of electron temperature ( $\bar{T}_e$ ), and this result is evident from tokamak experiments, spanning a wide range of  $\bar{T}_e$  values. PLT reports  $\gamma = 0.15$ , and JT-60 doubles this figure of merit to  $\gamma = 0.30$  when additional intense plasma heating is employed. Theoretical limitations to LHCD may restrict its use, however, to the low density and low temperature surface region of INTOR during full power operation.

On the other hand, good wave penetration and central current generation are possible with LHCD at very low density ( $< 10^{19} \text{ m}^{-3}$ ) on INTOR, which would permit current ramp-up prior to burn or quasi-steady state operation with periodic transformer recharging at low density between burns [4]. This LHCD option during low density transients implies the simultaneous presence of electric fields which drive additional Spitzer currents. The theory of LHCD combined with electric fields has been developed,[5] and data analysis shows the relevant experiments on PLT, ASDEX, and Alcator C are in good agreement with expectations.[6] Likewise JT-60 has shown partial transformer recharge while maintaining  $\sim 1$  MA of toroidal current.

Encouraged by the good agreement between theory and experiment it was decided during this phase to calculate the expected current drive performance for INTOR. A series of calculation tasks were defined, and all four INTOR participants were requested to carry out the analyses using their best national computation codes for a benchmark comparison. Four driver candidates were considered for this study: NBCD, LHCD, and FWCD at both high frequency ( $\sim \text{GHz}$ ) and low frequency (ICRF).



The first task was to compute the efficiency  $\gamma$  for steady state NCG at  $\bar{n}_e = 7 \times 10^{19} \text{ m}^{-3}$  and  $\bar{T}_e = 20 \text{ KeV}$ , requiring a centrally peaked current density and setting the electric field to zero.

For NBCD an impurity content with  $Z_{\text{eff}} = 2.0$  was specified, and  $\gamma = 0.37$  was found by the USA, with a deuteron energy  $E_b = 0.75 \text{ MeV}$ . This agrees very closely with the value obtained by most other INTOR participants (see Table II.1.4-1). A sensitivity study was done to infer the temperature dependence of  $\gamma$  for NBCD. For a fixed beam energy we found  $\gamma$  increases with  $\bar{T}_e$ , our results coinciding with the Japanese scaling,  $\gamma \approx 0.064 (\bar{T}_e/\text{keV})^{0.58}$ . The variation of  $\gamma$  with  $Z_{\text{eff}}$  is quite flat in the range  $1.5 \leq Z_{\text{eff}} \leq 3.0$ . We find  $\gamma$  has a maximum for  $E_b \geq 1.0 \text{ MeV}$ , and  $\gamma$  significantly deteriorates for  $E_b \leq 0.5 \text{ MeV}$ .

For LHCD it was not possible to generate a centrally peaked current density for the specified steady state INTOR plasma, due to the strong wave damping which prevents penetration beyond  $T_e \geq 10 \text{ keV}$ .

In contrast to LHCD, the fast wave may be accessible to the interior region of the INTOR plasma. In our work with high frequency FWCD [7] we chose a number of sources with frequencies from 0.3 to 1.0 GHz, and we tailored the power spectrum ( $1.6 \leq n_{\parallel} \leq 2.8$ ) to achieve a self-consistent MHD equilibrium with 3.62% beta and a smooth safety factor ( $q_{\text{axis}} = 1.01$ ,  $q_{\text{edge}} = 2.37$ ); the calculation was done with a noncircular cross section (elongation of 1.6) and for an aspect ratio of 4.2. The result with  $Z_{\text{eff}} = 1.5$ ,  $\gamma = 0.41$ , is within the range of values found by other INTOR participants (see Table II.1.4-1). At this beta value we find the temperature scaling is  $\gamma \approx .041 (\bar{T}_e/\text{keV})^{0.77}$ . In the range  $1.0 \leq Z_{\text{eff}} \leq 2.0$  we find  $\gamma \approx Z_{\text{eff}}^{-.373}$ . These sanguine findings for FWCD must be tempered with the knowledge that experimental evidence for FWCD is sparse, and there is concern especially at high frequencies that the fast wave may anomalously couple to the slow wave and suffer the same poor penetration experienced for high density LHCD.

On the other hand, at low frequencies the fast wave is well known from ICRH experiments to penetrate easily to the magnetic axis. The calculations of FWCD at these frequencies have not yet been refined, but, in agreement with the other INTOR participants, we find that centrally peaked current profiles are possible; for  $Z_{\text{eff}} = 1.5$  we compute  $\gamma = 0.33$ . For this calculation the frequency (64 MHz) was chosen such that wave damping and FWCD are achieved by

Table II.1.4-1  
 Benchmark Steady State  $\gamma$  [ $10^{20} \text{ A} \cdot \text{W}^{-1} \cdot \text{m}^{-2}$ ]  
 Values for  $\bar{T}_e = 20 \text{ keV}$ ,  $\bar{n}_e = 0.7 \times 10^{20} \text{ m}^{-3}$ ,  $E = 0$

Driver	EC	JAPAN	USA	USSR
LH $f = 2 - 10 \text{ GHz}$ $1.7 \leq n_{\parallel} \leq 4.0$ $Z = 1.5$	(0.5) <sup>a</sup>	(0.3) <sup>a</sup>	(0.3) <sup>a</sup>	(0.5-0.8) <sup>a</sup>
NBCD $0.4 \text{ MeV} \leq E_b \leq 0.7 \text{ MeV}$	0.39	0.37	0.37	0.5
HFFW $f = 0.3 - 1.0 \text{ GHz}$ $1.4 \leq n_{\parallel} \leq 2.8$ $Z \approx 1.5$	--	0.3, <sup>b</sup> ray tracing 0.6, <sup>c</sup> full wave	0.41	0.31 <sup>d,e</sup>
LFFW $f = 22 - 70 \text{ MHz}$ $3.0 \leq n_{\parallel} \leq 4.5$ $Z \approx 1.5$ , TTMP	--	(0.08) <sup>e,f</sup>	0.33	0.27 <sup>e</sup>

a - Centrally peaked current density not found at  $\bar{T}_e = 20 \text{ keV}$  if accessibility or frequency constraint is imposed.

b - Single pass result multiplied by  $p^{in}/p^e = (0.6)^{-1}$ , assuming multipass absorption.

c - Includes factor of 2.5 to account for 2-D velocity space.

d - Scaled by value at 15 keV by  $(20/15)^{0.34}$ .

e - Includes factor of 2.0 to account for 2-D velocity space.

f - Calculated at  $\bar{T}_e = 5 \text{ keV}$ ; uses  $n_{\parallel} = 12$ .

transit time electron pumping near the axis; only ~ 10% of the wave power is lost to second harmonic tritium cyclotron damping. Our ray tracing result is in rough agreement with the full-wave calculation done by the USSR (see Table II.1.4-1).

The second task addressed to the four national teams was to assess the possibility of controlling the current density profile by manipulating the parameters for the four candidate NCG methods. This exercise was motivated by observations that NCG can result in tokamak experimental operation with MHD properties differing from conventional ohmic performance [8]. Decoupling the current density and temperature profiles may eliminate sawteeth and perhaps permit operation at higher beta than is possible in the usual Troyon regime experienced with ohmic current generation. Both NBCD and FWCD were shown to allow current profile control. In the former case the best control was achieved by varying the height of the rectangular beam cross section; broad, or even hollow profiles are achieved with substantial injection into the relatively low density plasma well above/below the midplane, while more centrally peaked profiles result from injection concentrated near the midplane. The high frequency FWCD method provides the best profile control seen in our calculations. By launching a power spectrum rich in low  $n_{||}$  components centrally peaked currents were found. By shifting power to high  $n_{||}$ , hollow currents can be created. One example is in MHD equilibrium with a monotonic (single-valued) safety factor and a beta over twice the Troyon value. Indeed, FWCD should allow operation with  $q_{axis}$  well above unity, possibly permitting operation in the second stability regime.

Studies of profile control with FWCD in the ICRF have not yet been done. On the other hand, LHCD is presently felt to have little control flexibility, since it may be suited only for low density plasma regions. Hence, LHCD would necessarily be combined with some other driver if it were to be useful in this context.

The final task, which compared only LHCD and NBCD, was to calculate the power required to maintain 8 MA of current with a reverse electric field,  $E = -0.01$  V/m, assuming low density and temperature, as would occur during noninductive current ramp-up or transformer recharge. For this purpose we find LHCD is well suited: with  $\bar{n}_e = 4 \times 10^{18} \text{ m}^{-3}$ ,  $\bar{T}_e = 2 \text{ keV}$ , and  $Z_{eff} = 1.5$  we find a centrally peaked profile can be held in equilibrium with 24 MW of

power. Our result, which is somewhat pessimistic compared to the EC and USSR values (14 MW and ~ 20 MW, respectively), seems to be quite acceptable for an INTOR-sized tokamak. In contrast, NBCD for this application is less attractive. In order to avoid excessive shine-through at  $E_b \approx 0.5$  MeV it may be necessary to keep a higher density,  $\bar{n}_e \approx 6 \times 10^{18} \text{ m}^{-3}$ . Power balance considerations suggest  $\bar{T}_e \approx 6$  keV with NBCD under these conditions, and we find 34 MW is needed ( $Z_{\text{eff}} = 9$ ). Japan and the USSR are less optimistic on this issue, predicting 47 MW and 40 MW respectively, under similar conditions (but  $\bar{n}_e = 8 \times 10^{18} \text{ m}^{-3}$ ).

In an additional separate study we also considered the benefits of the neoclassical bootstrap current for reducing NCG power. According to theory a small seed current must be provided near the magnetic axis (e.g., by NBCD or FWCD), and the bootstrap current will then appear over the bulk plasma when the tokamak is in the banana regime. We calculated the FWCD efficiency,  $\gamma$ , without bootstrap contributions and the efficiency  $\gamma_B$  including bootstrap currents for identical MHD equilibria, and we studied the dependence of  $r \equiv 1 - (\gamma/\gamma_B)$  on tokamak parameters for a large variety of equilibria. Since we have  $\gamma_B = \bar{n}_e I R/P_B$ , where  $P_B$  is the (smaller) driver power required to achieve equilibrium with the aid of the bootstrap effect, we see  $\gamma_B > \gamma$ ; and  $r$ , which is the fractional reduction of driver power, will approach unity as the bootstrap effect predominates. If we define a peak poloidal beta  $\beta_{I0} = 2\mu p_0 / \langle B_p \rangle^2$ , we can fit our extensive calculations by the formula:

$$r \approx \begin{cases} C \beta_{I0} / (4\sqrt{A}) , & C \beta_{I0} / \sqrt{A} \leq 3.6 \\ 0.9 , & C \beta_{I0} / \sqrt{A} > 3.6 \end{cases}$$

The coefficient  $C$  is function of  $Z_{\text{eff}}$ , peak density and temperature, and the plasma profiles. (Details of this work will be published separately.) For INTOR with congruent profiles ( $d\ln T/d\ln n = 1$ ) we find  $r \gtrsim 0.9$  at high density ( $\bar{n}_e = 1.4 \times 10^{20} \text{ m}^{-3}$ ), which requires FWCD with only  $P \approx 10$  MW. While this very modest amount of external power would make steady state operation quite attractive, we caution that flatter density profiles will significantly reduce  $r$ . By varying the density/temperature profiles we found that  $r \lesssim 0.5$  would be likely for flatter density profiles. We should point out that the bootstrap current may be particularly relevant to steady state INTOR operation in light of the positive experimental results seen lately on TFTR [2].



## 1.5 Electromagnetics

For the design of poloidal field (PF) coil systems which are consistent with a chosen plasma configuration, it is desirable to identify coil locations which minimize the poloidal field energy. Several optimization codes exist which can solve this generalized free-boundary Grad-Shafranov equilibrium problem. However, at several of the past INTOR workshops, discrepancies have been noted between INTOR delegation predictions for the coil currents necessary to produce a given plasma configuration. To understand the source of the discrepancies, some benchmark equilibrium calculations were performed. The plasma shape, current profile, and beta were precisely defined, and the positions of the poloidal field coils were given. Minimum energy PF coil currents were sought which produced the specified equilibrium configuration (the actual plasma boundary being fit to the desired shape in a least squares sense). When results were compared with the various delegations, good agreement was consistently found, giving confidence in the validity of the computer codes. The previously obtained discrepancy in results is understood to be due in large part to the sensitivity of the required PF coil currents to the assumed plasma beta and plasma current profile. The beta dependence arises because although the primary role of the outer PF coil nearest the midplane is to provide the vertical field for radial equilibrium, this coil also provides significant voltseconds. The higher the beta the more voltseconds are provided, therefore calculations performed at fixed voltseconds give rise to different PF coil currents when beta is varied. It is also found that the dependence of required coil current on plasma current profile can be sensitive. Simulations performed for an early CIT design (major radius 1.75m, minor radius 0.55m, plasma current 9.0MA), for example, indicate that varying the plasma  $i_{li/2}$  from 0.30 to 0.50 can change the location of the null point by several centimeters. Calculations which constrain the shape to be constant must compensate for this change by adjusting the coil currents appropriately.

The Electromagnetics Group has considered the impact of maintenance scheme (horizontal versus vertical access) on the PF configuration and magnetic energy. A highly elongated plasma requires a vertical field whose curvature is such that the field index is negative. The most natural location for a vertical field coil is therefore near the equatorial plane. If the primary vertical field coil has to be placed at some distance,  $\Delta z_{coil}$ , from the midplane, the vertical field seen by the plasma is weighted by the cosine of the angle between the equatorial plane and line from the plasma to the coil. As  $\Delta z_{coil}$  increases, the coil current must increase to give the same vertical field. Moreover, the same coil now contributes some higher order multipole (shaping) component, which can interfere with the shaping component of the main divertor coil. Both of these effects tend to increase the magnetic field energy and total megamp-meters, which are found to be sensitive functions of  $\Delta z_{coil}$ . No matter what maintenance scheme is chosen, the existence of an auxiliary heating port imposes an exclusion zone for the placement of PF coils close to the midplane. The actual size of this zone depends on design details. In a vertical maintenance scheme, the size of the heating port is the main determinant of the outboard exclusion zone, whereas, in a horizontal



maintenance scheme, the outboard exclusion zone can be expected to be larger. Since the PF energy depends sensitively on  $\Delta z_{\text{coil}}$ , it is not possible to argue strongly in favor of one scheme compared with another, because minor changes in the assumptions of the size of the exclusion zone can alter the conclusion. As a general principle, it is advantageous to minimize  $\Delta z_{\text{coil}}$ .

Considerable progress has been made in the development and benchmarking of the Princeton Tokamak Simulation Code (TSC). This free boundary axisymmetric simulation code was developed to model the transport time-scale evolution and/or the positional stability and control properties of noncircular tokamaks. The validity of TSC has been tested against various analytical plasma models, but more importantly, has been validated by comparison of code predictions with controlled experimental shots from PBX, TFTR, and DIII-D. In addition, the code has been used to simulate the plasma behavior during a major disruption on TFTR where current quench decay rates of approximately 1 MA/msec were experimentally observed. Code developments include (1) the implementation of an improved feedback capability allowing realistic modeling of most tokamak control systems, (2) the capability of modeling a time varying toroidal magnetic field, allowing it to be simultaneously ramped with the toroidal current, and (3) the inclusion of alpha particle heating terms in the transport section of the code, which allows the modeling of ignition experiments. The TSC has been used to model the current ramp and burn phases of the proposed CIT experiment, and has been useful for examining the voltsecond requirements.

The results of simple models for predicting wall loads during major plasma disruptions show that results can be very sensitive to the assumptions regarding the action of the plasma during a disruption. Typically, in the simple models the plasma current is assumed to ramp linearly to zero in a given time, at a fixed location, or else the plasma is forced to move along some predetermined trajectory while the current is quenched. The sensitivity of the results to the assumptions shows the need for using codes which treat the plasma and its interaction with external magnetic fields in a more consistent way. The TSC has been used to simulate several disruptions on TFTR and on DIII-D. Since the code incorporates a detailed transport model the thermal quench phase of the disruption can be simulated, as well as the subsequent current quench. When model parameters are chosen appropriately, the results of the TSC have been shown to agree well with the experiments. The DSTAR computer code has been developed at the IDAHO National Engineering Laboratory and couples the TSC with other packages which quantify the surface erosion and induced forces which occur during major plasma disruptions. DSTAR has been used to predict current quench rates, and thermal and mechanical loads in the FW/B/S for INTOR. The rates are found to be sensitive to the disruption scenario, and can be particularly high if the internal disruption follows a vertical instability. The reason here is contamination of the plasma from impurities when the disruption occurs while the plasma is close to the divertor plate. The predicted current quench rates can be as high as 3MA/msec. There are uncertainties in the modeling parameters used to simulate the disruptions, but it is believed likely that current quench rates well in excess of 1MA/msec will

occur.

Operating scenarios for INTOR have considered the use of separate control coils to provide active vertical stabilization of the plasma. A rapid vertical plasma displacement would be initially restrained by fields due to eddy currents induced in passive conducting structures; then the active coils would be excited to provide the required stabilization field. By using a static plasma model with a variable current density, "contours of constant effectiveness" of passive material can be traced which indicate where the placement of conducting material is most effective in stabilizing the vertical motion of the plasma on the ideal timescale. When the location of these contours is compared with an outline of the INTOR baseline design, it is found that the most effective material is on the outboard side. Although the bulk of the conducting material in the machine is ineffective, we have concluded that no additional passive coils need to be incorporated into the design. This result is in agreement with earlier results which employed a more elementary treatment of the plasma as a single current filament.

The PF coil system for the baseline single null INTOR configuration has been optimized relative to the OH flux swing bias at start-up and at end-of-burn by studying the sensitivity of selected PF design variables (stored energy, ampere-meters, coil current density and maximum magnetic field) to chosen biases. The central solenoid current density and maximum field levels are the most strongly dependent variables, and set the optimum swing to be from +46 to -66 vsec for a total of 112 vsec provided.

The principal innovation recommended to the INTOR study is the incorporation of high current density, high field superconducting magnets. When combined with improved radiation tolerance of the magnets to minimize the inner shielding of the tokamak, a substantial reduction in machine dimensions and capital costs can be achieved. Cable-in-conduit conductors (CICC) are capable of the desired enhancements and are under development. Because conductor stability in a CICC depends more on the enthalpy of the interstitial helium than the copper resistivity, high stability is retained at current densities of the order of  $40 \text{ A/mm}^2$  and fields as high as 12 T, even with high heat loads. Radiation damage to the copper stabilizer is less important because the growth in resistance is a second order effect on stability. Such CICC conductors lend themselves naturally to niobium-tin utilization, with the benefits of the high current-sharing temperature of this material being used to advantage in absorbing radiation heating. The constraints on current density imposed by protection criteria must still be met, but these are ameliorated by the selection of higher operating current (made feasible by a wind-and-react fabrication technique). In this way it is possible to consider both higher fields and current densities for INTOR.

Peak nuclear heating rates above  $5 \text{ mW/cm}^3$  are cryogenically acceptable with large refrigerators. This corresponds with neutron fluences of about  $10^{19} \text{ n/cm}^2$  or insulator radiation

doses of  $10^{10}$  rads in  $10^8$  seconds. These values are compatible with next generation engineering test reactors if radiation resistant polyimide insulators are used to provide the main voltage standoff.

The radial build out to the inner first wall when coupled with the physics requirements for good performance sets the major radius of the tokamak. Minimizing the radial build by the use of higher current densities and allowing higher heat loads can be a major factor in reducing the size and hence cost of INTOR.

## 1.6 Configuration and Maintenance

The critical issues and innovations dealing with Configuration and Maintenance consisted of six tasks. These were the following.

1. Comparative study of vertical and horizontal access configurations,
2. use of shape memory alloys,
3. ferromagnetic inserts for ripple reduction,
4. PF coil redundancy,
5. rapid replacement schemes for the divertor and first wall, and
6. containment of tritium and activated dust.

Tasks 1, 5, and 6 were from the original critical issue work, and tasks 2, 3, and 4 were recommendations from an INTOR Specialists Meeting on Innovations held in January 1986. Task 1 is the most significant since the choice between vertical or horizontal has the greatest impact on the configuration design and the maintenance approach. A summary discussion for each of these follows.

### 1.6.1 Vertical and Horizontal Access Configurations

The INTOR configuration is based on the horizontal removal of torus sectors, including the biological shield, for the replacement of first wall and blanket components. The comparative study between this approach and the vertical approach is based on a configuration similar to the Next European Torus (NET), whereby first wall-blanket components are removed in a vertical fashion. The primary difference between these configurations is the location of the poloidal field (PF) coils and the emphasis of the maintenance philosophy. The INTOR design was initially developed with simplified maintenance as the primary objective, i.e., straight, radial extraction of complete torus sectors. This led to a configuration where the PF coils were positioned to provide a large window opening for the sector without considering the impact to the cost of the PF system. The vertical access design, shown in Fig. II.6.1 as a modification to the INTOR baseline, has PF coils located to provide a small horizontal window for heating and test modules and a vertical access port for removal of first wall-blanket components.

A comparison of these approaches showed that the latter design had a 25 percent reduction in the cost of the PF coils; however, most of that reduction was the result of reducing the diameter of the lower outboard coil. The cost reduction contribution from relocating the other coils was approximately 7 percent. This modest reduction is the result of a low plasma elongation of  $k = 1.6$ . Further study showed that for elongations  $\geq 2.0$ , PF cost reductions are substantial.



Time and motion studies for replacing first wall-blanket components did not reveal any substantial difference in the maintenance time required. Both approaches were within 10 percent of each other for downtime. Also, it does appear possible to vertically remove internal reactor components without disturbing peripheral equipment like heating modules and test modules. While this is clearly an advantage, vertical removal requires a greater number of first wall-blanket segments and complex handling equipment. The configuration shown in Fig. II.6.1 has 48 blanket segments corresponding to 12 torus sectors. The greater number of segments require a more complex arrangement of cooling pipes, and the greater number of surface gaps and mechanical connections will reduce the effective blanket surface available in the torus.

Based on the level of design detail to date, it appears that both approaches are feasible. For higher elongation plasmas, a vertical access approach with "optimized" PF coil locations should be pursued in conjunction with developing feasible segmented blanket designs.

### 1.6.2 Shape Memory Alloys

Shape memory alloys (SMA) are widely used for hydraulic pipe couplings and appear suitable for vacuum joints. These alloys are based on compounds of nickel and titanium and derive their shape-memory properties from austenite/martensite transformations which are a function of temperature. Couplings made from these compounds are simpler and faster to make than alternatives such as welding. SMA applications for INTOR are proposed for cooling pipe connectors, mechanical quick-connectors, and metal packing for vacuum seals.

The unique aspect for INTOR applications is the neutron environment. Results from tests in Japan using fast neutrons (0.1 MeV) at 323°K at a fluence of  $8 \times 10^{19}$  per  $\text{cm}^2$  presented no problems, indicating that SMA could be used outside the INTOR shield. Recent work at Oak Ridge National Laboratory (ORNL) using ion bombardment to predict the effects of fluence and temperature indicate that SMA may be used behind the blanket structure.

The use of shape memory alloys will not impact the configuration, but they have the potential to reduce the downtime for certain maintenance operations. In particular, they are suited for unexpected repairs in areas with limited access.

### 1.6.3 Ferromagnetic Inserts

Ferromagnetic inserts located in front of the toroidal field (TF) coils effectively reduce the toroidal field ripple. The magnetic flux produced by the inserts increases the field in the plasma region between coils and reduces the field in the plane of the coils. This reduction of field ripple makes it possible to reduce either the number of TF coils or their size.

Analysis shows that it is possible to reduce the outer leg of the INTOR coils by 0.5 m radially. However, from a maintenance point of view, access to the torus is correspondingly reduced. On the other hand, a reduction in the number of coils from 12 to 10 results in a proportionate increase in midplane toroidal access. This can be achieved by incorporating the ferromagnetic material into the torus shield and, since the shield is already a substantial structure, reacting the electromagnetic forces should be manageable. These forces can be as high as 20 MN.

#### 1.6.4 PF Coil Redundancy

Untrapped poloidal field coils are the basis of the PF system in the reference design. However, the cost penalty for the lower outboard coil weighing 600 tonnes is approximately 18 percent compared to a more natural position closer to the plasma under the TF coils. A failure of this coil in its optimized position requires a major disassembly of the reactor. Hence, it requires extreme reliability or built in redundancy.

High reliability may be achievable by making the coil larger and operating it at reduced current density. Redundancy may be achieved by installing spare coil segments with independent leads and structure. In the first approach, present technology cannot guarantee faultless operation. For the second, the questions are how many spare segments are needed, and how much space can be devoted to additional leads and structure.

An approach that appears satisfactory compared to the present baseline is to locate the lower outboard coil in its optimum position under the TF coils. In addition, during construction, provisions for the large trench (as in the baseline) should be incorporated into the reactor hall. In the event that this trapped coil should fail, it can be abandoned in place and a larger, less efficient coil can be installed in the trench as in the baseline. The impact to reactor downtime for coil replacement will be the same, since in the present baseline a spare coil has not been assumed. If the trapped coil does not fail, a substantial cost benefit results from the reduced PF system cost. The downtime to replace a lower outboard coil may approach three years; one year to procure material, one year for winding and testing, and six months to one year for coil installation and resumption of reactor operations.

#### 1.6.5 Rapid Replacement for Divertor/First Wall

Rapid replacement of these in-vessel components was based on maintaining the vacuum integrity of the plasma chamber. The present baseline requires a detritiation bakeout that has been estimated at one week and a plasma chamber reconditioning also for one week. Therefore, if these components can be replaced under vacuum conditions, a significant saving in downtime is possible. Figure II.6.2 shows a concept for remotely replacing divertors using this approach. The design incorporates isolation valves and a spare divertor module. Since the divertors are estimated to require annual replacement, the downtime savings will offset the cost of developing this equipment.

This is not the case for evacuated structures for replacing torus sectors. Each sector is approximately  $4 \times 7 \times 5$  m, hence the containment structure is an unreasonable size and will impact the reactor hall size. In addition, the INTOR first wall is considered to be a lifetime component, therefore, any replacements will be unscheduled and infrequent.

#### 1.6.6 Containment of Tritium and Activated Dust

Bakeout for detritiation and in-vessel cleaning for the collection of solid particulates will be required before opening the plasma chamber. Reduction of secondary outgassing and activated dust may be accomplished by maintaining a slightly negative pressure in the torus with the use of the



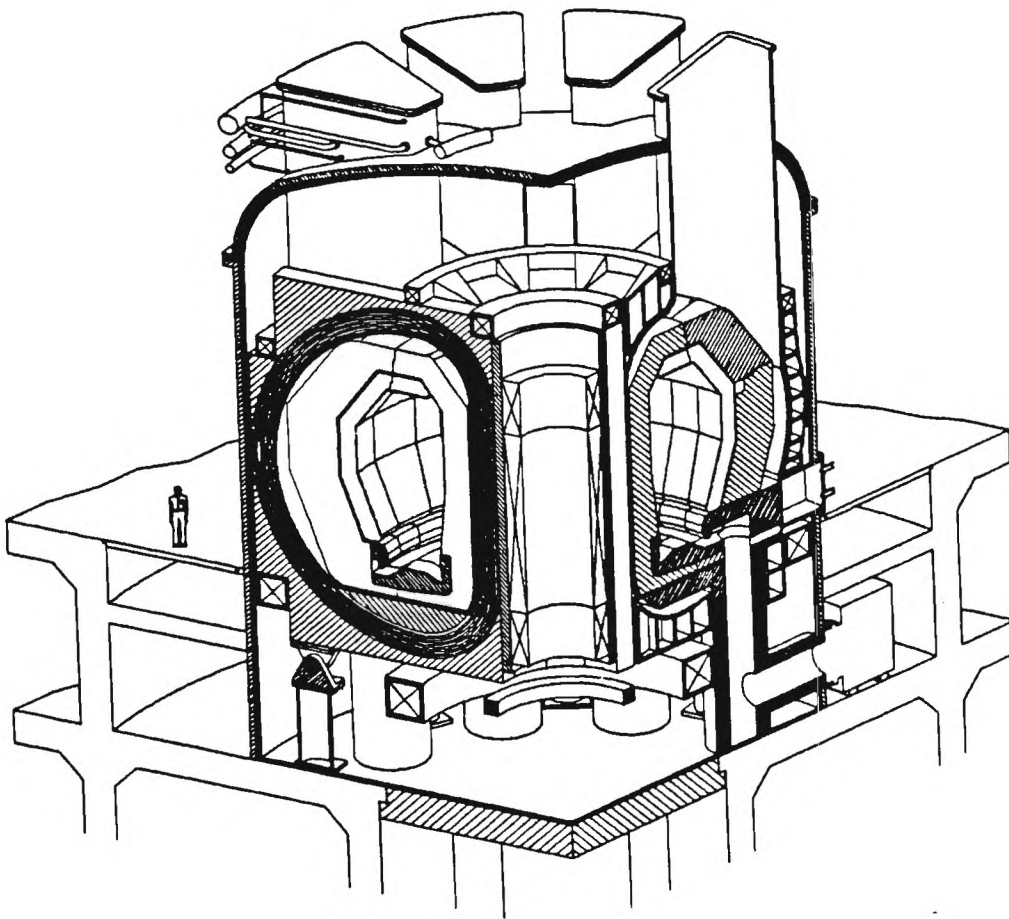


Fig. II.6.1. INTOR concept based on vertical access for replacing first wall-blanket components.

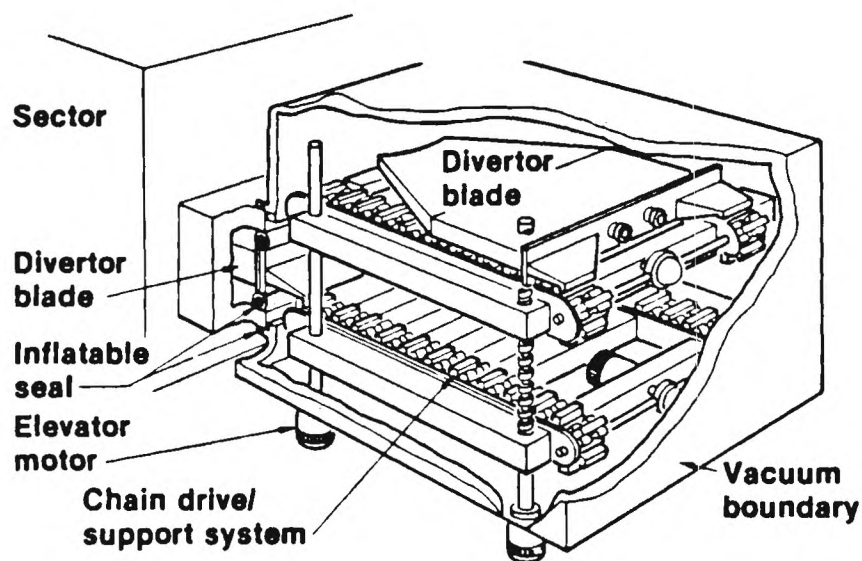


Fig. II.6.2. Containment concept for remote replacement of a divertor module.

vacuum pumping system. Replacement of components like test modules or divertors, using equipment like that shown in Fig. II.6.2, automatically provides containment. Large components such as a torus sector may be extracted into shroud-like containments, although additional study for this approach is needed to determine if particulate afterheat will damage these flexible structures.

## **1.7 Blanket and First Wall**

This phase of the Blanket and First Wall study was focused on the following four areas:

- An update of critical materials data base for INTOR.
- First wall design and performance analysis.
- Development of blanket concepts capable of providing tritium self-sufficiency.
- Recommended materials and nuclear technology R&D.

### **1.7.1 New Materials Data Base**

New materials data have been reviewed on austenitic and ferritic steels, graphite and C/C composites, ceramic breeder materials, liquid breeder materials, divertor materials, and magnet materials.

#### **Austenitic Steels**

Additional information on three critical issues for austenitic steels was presented: (1) the sensitivity to aqueous stress corrosion, (2) low temperature radiation effects on mechanical properties, and (3) effect of radiation on weldments. These new data show: aqueous stress corrosion cracking of austenitic steels, particularly in the presence of irradiation, is identified as a serious feasibility issue for the reference INTOR first wall/blanket structure. Significant loss of tensile ductility is also a major concern. Austenitic stainless steel is the only reasonable structural material for the low temperature first wall and blanket of INTOR.

#### **Ferritic/Martensitic Steels**

The selection of ferritic/martensitic steel as the first wall/blanket structure for the low temperature, cyclic operating conditions of INTOR is not recommended. The DBTT of ferritic steels is increased more than 200°C by low temperature (< 300°C) irradiation. The effect of hydrogen is of particular concern at the low temperatures where release of the internally generated hydrogen may be inhibited. The hydrogen effect may be even more critical for irradiated material, e.g., ΔDBTT, and/or for weldments.

### Graphite and C/C Composites

Three aspects of graphite and C/C composites, viz., form of redeposited material, radiation effects, and tritium retention have been evaluated. The effect of high helium generation rate (He/dpa ~ 300) is unknown but may be significant at low temperatures (< 1200°C). The C/C composites provide significant tensile strength and fracture toughness advantage; however, they are predicted to be significantly less radiation damage resistant because of the large anisotropy of the fibers compared to nuclear graphites.

### Breeder Materials

Significant R&D efforts have been conducted in recent years with emphasis on the candidate ceramic breeder materials:  $\text{Li}_2$ ,  $\text{LiAlO}_2$ , and  $\text{Li}_4\text{SiO}_4$ . Mass transfer/weight loss of  $\text{Li}_2\text{O}$  in flowing He at low moisture contents is a concern. Tritium release rates from ceramic breeders are sensitive to grain size and temperature. Small grain size in  $\text{LiAlO}_2$  is especially critical because of the low tritium diffusivity. At sufficiently high temperatures or small grain size, most of the tritium should be released from all candidate ceramic breeder materials. There is a serious concern regarding stress corrosion cracking of austenitic steels by Li-salts and of tritium recovery from the salt.

### Divertor Materials

Primary candidate materials include tungsten plasma facing materials bonded to copper heat sink. Liquid metals and He-burial concepts have been proposed as innovative divertor target materials. Vanadium, nickel, and iron are candidate materials for He-burial concept. The minimum energy for effective helium trapping (~ 30 at.% trapping fraction) is estimated to be ~ 30-50 eV. Analyses performed indicate that lithium and tin may be acceptable liquid metal divertor targets.

### Magnet Materials

The radiation limits for  $\text{Nb}_3\text{Sn}$  are estimated to be ~  $1 \times 10^{19} \text{ cm}^{-2}$ . The dose limits for epoxy insulators and polyimide insulators are predicted to be in the range of ~  $1 \times 10^9 \text{ rad}$  and ~  $1 \times 10^{10} \text{ rad}$ , respectively, depending on the shear stress requirements.

### 1.7.2 Disruption Analysis

Since disruptions have a major influence on the design and performance of the first wall and divertor, special emphasis has been placed on analyses of these effects. A parametric erosion analysis has been performed for the first wall and divertor materials for a range of conditions. This analysis considered disruption times of 0.1 to 20 ms deposited energy densities of ~ 100 - 1000 J/cm<sup>2</sup> on stainless steel, graphite, and tungsten. The extent of vaporization, melt layer thickness for the metals, and effects of vapor shielding have been determined. Based on a tentative disruption scenario, in which the thermal quench is assumed to occur in ~ 0.1 ms with most of the energy going to the tungsten divertor plate, the predicted lifetime erosion of the tungsten is ~ 17 mm and that of the steel wall is ~ 1.7 mm. For this case the melt layers are assumed not to erode in the short disruption times.

Analyses conducted indicate that surface cracking of a steel wall will occur as a result of severe disruptions; however, propagation of the crack will not occur, and hence, the normal fatigue life will not be significantly degraded.

### 1.7.3 First Wall Designs

The first wall design activity was concentrated on evaluation of critical issues associated with a steel wall and a graphite protected wall. The steel wall concept provides significant advantages with respect to design simplicity and lifetime under normal operating conditions. The primary concerns relate to vaporization and melting of the surfaces during a disruption. A graphite liner will provide protection from the severe disruptions; however, additional problems exacerbated during normal operation relate to more complex design, tritium retention in the graphite, and a limited radiation lifetime. A revised plasma disruption scenario developed by the physics groups during this phase has major implications regarding first wall design.

Three first wall design concepts have been considered for in-depth analyses using the modified INTOR design parameters to define their performance characteristics and identify unresolved design issues. These analyses cover a wide range of reactor parameters including the reference operating conditions as given in Table II.1.7-1. The three designs have a water coolant with a Type 316 SS structure. The first concept consists of a

bare stainless steel water cooled panel. The thickness of the panel facing the plasma is limited by thermal stress and/or fatigue criteria. The second concept uses a grooved structural wall to allow a higher erosion rate and surface heat flux relative to the first concept. The third concept has a radiatively-cooled tile, viz., graphite or C/C composite, on the plasma side which will accommodate more severe disruption loads.

TABLE II.1.7-1  
INTOR Parameters for First Wall/Blanket/Shield Analyses

Average neutron wall load	1.3 MW/m <sup>2</sup>
Maximum surface heat flux to first wall	0.2 MW/m <sup>2</sup>
Availability	25%
Number of cycles	$2 \times 10^5$
Cycle burn time	$\geq 200$ s
Cycle time	$\geq 270$ s
Number of major disruptions	200-1000
Peak disruption energy to inboard first wall	175 J/cm <sup>2</sup>
Time for energy deposition per disruption	2 ms
Sputtering erosion of SS from first wall	$\approx 0.2$ mm/MW $\cdot$ Y/m <sup>2</sup>
Tritium breeding blanket coverage	0.6-0.8

The bare stainless steel first wall is recommended as the reference for the INTOR design. The primary advantage of the bare steel wall includes design simplicity and a well-established data base. Key issues identified for further study include: (1) effectiveness of vapor shield during disruptions, (2) effects of disruptions on fatigue life, (3) melt layer stability during disruptions, and (4) advantages and disadvantages of cold-worked versus solution annealed stainless steel, particularly as affected by welding/joining. For bare first wall designs with a fatigue lifetime of  $2 \times 10^5$  cycles, the allowed peak nominal heat fluxes are  $\sim 0.4$  MW/m<sup>2</sup> for a thickness of  $\sim 6$  mm. A thicker grooved wall will provide additional ruggedness.

#### 1.7.4 Tritium Breeding Blanket

The primary objective of the blanket activity was to investigate the feasibility of providing tritium self-sufficiency without compromising the



reactor design and reliability and with modest R&D requirements. Although several blanket concepts were examined the analyses were focused primarily on two concepts: (a) a water-cooled, ceramic breeder concept, and (b) an aqueous/salt self-cooled concept. Both concepts utilize an austenitic steel structure, incorporate substantial amounts of beryllium to enhance the tritium breeding performance and operate with low temperature ( $\sim 100^{\circ}\text{C}$ ) coolant.

The main function of the INTOR blanket is to produce the tritium required for the operation with minimum first wall coverage. The blanket extrapolation to commercial power reactor conditions and the proper temperature for power extraction have been sacrificed to achieve the highest possible local tritium breeding ratio (TBR) with minimum additional R&D and minimal impact on reactor operation. In addition, several other factors have been considered in the FWBS study including safety, reliability, lifetime, fluence, number of burn cycles, simplicity, cost, and development issues. A set of blanket evaluation criteria has been compiled to compare possible INTOR blanket concepts.

The proposed INTOR blanket is an  $\text{H}_2\text{O}$ -cooled, He-purged system with layers of SS structural material, Be multiplier,  $\text{LiAlO}_2$  breeder, and C reflector (Fig. II.1.7-1). The first wall surface area for INTOR is  $380\text{ m}^2$  with  $230\text{ m}^2$  ( $\sim 60\%$ ) coverage by the blanket. The total thickness of the breeder layers is  $\sim 60\text{ mm}$ , giving a breeder volume of  $13.8\text{ m}^3$ . The total thickness of the Be layers is  $\sim 240\text{ mm}$ , giving a multiplier volume of  $55.2\text{ m}^3$ . Assuming that the Be is at 70% of its theoretical density and the breeder is at 80% of its theoretical density gives masses of 71.4 Mg for Be and 28.9 Mg for  $\text{LiAlO}_2$  (22.3 Mg for  $\text{Li}_2\text{O}$  and 26.7 Mg for  $\text{Li}_4\text{SiO}_4$ ).

Key design features for the water-cooled solid breeder blanket are given in Table II.1.7-2. It is concluded that tritium self-sufficiency is readily attainable if the key materials feasibility issues, viz., aqueous stress corrosion and loss of fracture toughness of austenitic steel, can be favorably resolved.



### 1.7.5 R&D Needs

Critical materials and technology R&D needs for INTOR first wall, blanket, divertor, and shield have been defined. The most important feasibility issues are:

- aqueous stress corrosion of austenitic steel,
- effect of radiation on low-temperature fracture toughness of austenitic steel,
- radiation effects on graphite and C/C composites (including helium).

### 1.8 Additional Physics Issues

One topic was covered in this area: the fast alpha particle loss due to toroidal field ripples. The mechanisms of ripple trapping and ripple-induced diffusion of banana orbits (stochastic diffusion) were studied. For ripple values around 1% (peak-to-average), the latter mechanism is the dominating one. It is estimated that for INTOR about 2% to 3% of the fusion alpha energy and about 4% to 7% of the fusion alpha particles are lost through this mechanism. It is shown that the alpha particle flux to the wall is localized between the TF coils and displaced from the mid-plane at small poloidal angles. However, these results are different from the results produced at JAERI recently, which indicated losses more than 3 times the above values.

Comparison of the models and the numerical procedures used in these computations has identified apparently important differences. These include differences in the numerical integration approaches, in approximations of the scattering operator of the charge particles, and in the presence of an artificial speed up of the time scale of integration. Work is needed to resolve these discrepancies, and to test the results in experiments.

## 1.9 Additional Engineering Issues

There are two topics covered in the area of additional engineering issues: these include compact reactor concepts as tokamak concept innovations and engineering scoping studies performed in anticipation of a design upgrade of INTOR.

### Compact Reactor Concepts

A special task addressed in the INTOR Workshop was innovations that would significantly improve the prospects of tokamak development leading to an attractive, viable tokamak fusion reactor.

The U.S. generated numerous ideas for consideration; several of these included compact reactor concepts. Two ideas using copper coils were advanced. The first of these is the spherical torus, which is a very small aspect ratio confinement concept obtained by retaining only the indispensable components, such as the toroidal field coils inboard to the plasma torus. This concept is characterized by high toroidal beta (greater than 0.2), naturally large elongation (greater than 2), large plasma current (greater than 7 MA/mt), strong paramagnetism, and strong magnetic helical pitch. This concept has features which combine to produce a spherical torus plasma in a unique physics regime that permits compact fusion at low field and modest cost. The second concept is the elongated tokamak concept which calls for extreme shaping of the plasma by elongation (values greater than 4). Benefits associated with this concept include good confinement, high beta, and high plasma current density at moderate magnetic fields and stresses. The high current density suggests the capability to ohmically ignite. Maintenance and repair are facilitated using rapidly demountable toroidal field coils.

Two ideas using superconducting magnet systems were also suggested. The first is an all-superconducting, steady-state tokamak based on a minimum major radius and strong plasma shaping. This concept relies on high magnet current densities, high-field plasma shaping coils, minimum neutron shielding, and steady-state operations assuming current drive. The resulting design achieves high beta conditions in the first stability regime in a very compact device with associated modest cost. The concept is dependent upon the development of efficient current drive methods. The second superconducting concept is the microwave tokamak. This idea seeks an attractive high Q, steady-state reactor in which the total plasma current is driven noninductively by a combination of ECH, wall reflection of synchrotron emission, and bootstrap current. The microwave sources need further development for this concept application.

### Engineering Scoping Studies

A series of scoping studies was performed to aid in the eventual update of the INTOR design. These studies were initiated as a means of learning which of many possible changes to the design would seem to be feasible, practical, and would have a significant impact on the overall design and performance.



A set of recommended scoping studies was developed by all of the international participants. This recommended set of studies included the following elements:

- Reduction in size and/or number of TF coils
- Single vs double-null divertor
- Noninductive current drive
- Quasi-steady-state operation
- Pumped limiter with ergodic edge
- Combined use of NBI for heating, current drive, and impurity flow reversal
- Pusher coil for higher beta
- Higher plasma current
- Integration of the set individual elements

In addition to this set of recommended elements, additional studies were performed in the U.S. to examine the impact of varying certain parameters and also to develop a set of integrated point designs to illustrate possible upgrades that could be considered for INTOR.

These scoping studies were performed using the Fusion Engineering Design Center Tokamak Systems Code. This code has been used in numerous previous U.S. design studies and upgraded with time and application. The code has the ability to incorporate a large number of physics and engineering variables and constraints. A distinguishing feature of the present version is the ability to simultaneously iterate on many variables to achieve a converged solution for a selected figure-of-merit.

The results of this study identified (1) several high sensitivity areas where significant impact can be made on the design, and (2) several representative integrated design concepts that indicate varying degrees of improvement that can be made to the INTOR design by making the indicated choices in configuration or engineering.

The major items that have a significant impact in reducing the major radius are:

- Increasing the elongation (to values in the range 1.9 to 2.2)
- Use of noninductive current drive (which permits reduction in the size of the solenoid)
- Reduction of the inboard plasma scrape-off thickness
- Increase in the plasma operating temperature (to the range of 15 to 20 keV)

- Reduction of the inboard shield thickness
- Using higher overall TF coil current density at a given field level to effect a reduction in the TF coil thickness

The results of these scoping studies provide a quantitative basis and insight for potential changes to improve the INTOR design concept.

## 2. ANALYSIS OF INTOR-LIKE DESIGNS

### 2.1 Introduction

The International Fusion Research Council (IFRC) recommended that the INTOR Workshop conduct, during 1987, critical analyses of existing INTOR-like designs, with the aim of preparing a useful information base for future design work for the Engineering Test Reactor (ETR). As a first step, members of the INTOR, FER (Japan), NET (EC), OTR (USSR) and TIBER (USA) design teams met together in an IAEA Specialists' Meetings to document in a common format, discuss and compare the programmatic and technical objectives, the engineering and physics design constraints (i.e. physical limitations such as stress limits, beta limits), the main features which drive the design concept (i.e. choices made by the designers such as to incorporate non-inductive current drive or a horizontal maintenance and assembly scheme), and the design specifications (e.g. major parameters, choice of materials, choice of heating method) for the five designs. These topics were further analyzed during the course of the INTOR Workshop.

There is a great deal of similarity in objectives among the five designs. Achievement of reactor relevant plasma operating conditions, incorporation of reactor relevant technologies in the machine components, and provision for engineering testing are broad, common objectives. All the designs are predicated upon a start of construction of about 1993.

There are some differences in objectives, however. The fluence objective varies from  $0.3 \text{ MW}\cdot\text{a}/\text{m}^2$  for FER to  $5.0 \text{ MW}\cdot\text{a}/\text{m}^2$  for OTR, with associated variations in materials and components testing capabilities and availability requirements. Ignition is an objective for FER, INTOR and NET, while steady

state operation at  $Q > 5$  is an objective for TIBER, and OTR has a high- $Q$  objective. Tritium self-sufficiency is an objective for OTR, while FER will not breed any tritium except in test modules. OTR is the only design with a nuclear fuel production demonstration objective.

There is also a difference in the objective of the design studies, as distinct from the objectives of the devices, which has caused differences in the designs. The TIBER design activity had as an objective to study the extent to which a compact design could be achieved by making aggressive assumptions about the development and incorporation of new technologies which are yet to be developed.

### 2.3 Physics Constraints

The physics assumptions and constraints for each of the four national ETR designs and INTOR are quite similar (Table II.2.3.1. The differences in the designs are mainly due to the choice and emphasis of different features (see Sect. 2.5) and the use of different engineering constraints (see Sect. 2.4). On the whole, the national designs tended to adopt more conservative physics assumptions than INTOR, especially with regard to  $\beta$  and  $q_{\text{edge}}$ . All of the designs rely upon H-mode confinement and have incorporated an open poloidal divertor for this. In addition, they rely upon current scaling for confinement and beta with the result that the specified currents are in the 10 MA range. The plasma is elongated to achieve this current. The elongations vary from 1.5 to 2.4. All of the designs have adequate margin for ASDEX-H scaling, but none of the designs can ignite with most L-mode scalings.

All of the designs rely upon densities for ignited operation that are at the high end of the present tokamak data base. The designs utilizing current drive with subignited operation can afford more conservative assumptions with respect to the density limit. The Murakami parameters range from 15 to 25 for ignited operation and  $\sim 8$  for  $Q = 5$  operation.

All of the designs use a "Troyon" type of scaling for the beta limit, although the choice of the Troyon coefficient is somewhat different in each design. As stated before, this type of scaling leads each design to emphasize increased current as a way to maximize beta.

The edge safety factor varies among the designs but the cylindrical safety factors are very close for all of them.

All of the designs rely upon the operation of an open, high recycling divertor to provide power and particle exhaust. Advanced fueling techniques, including high velocity pellets and other schemes, have been considered by all of them.

A toroidal field ripple in the range of 0.75 to 1.2% is anticipated to be adequate for fast alpha particle confinement, although major uncertainties remain.

The physics assumptions for current drive and heating are quite similar among the designs. For those that do not rely upon current drive, ICRF is generally the heating method adopted as far as a choice has been already made. Where current ramp-up and transformer recharge is used, lower hybrid wave heating is the method of choice. Those designs incorporating steady-

### 2.3 Engineering Design Constraints

Engineering constraints are those parameters and limits used in a design that are derived primarily from physical laws of nature and over which the designer has limited choice. For example, these include such elements as the radiation damage limits, heat load limits, etc. In addition, choices made in one system or aspect of a design can then pose as a design limit to be satisfied by other systems or aspects of the design. For example, the decision to use a double null, highly elongated plasma poses limits on the mechanical configuration which must be satisfied.

In the engineering category, the design constraints were arranged in three groupings: mechanical and configuration; electromagnetics, heating and current drive technology; and nuclear.

In the mechanical and configuration grouping, the major engineering design constraints and the range of choice used in the five designs are as follows:

Magnet configuration: Placement of all coils in a common cryostat or placement of magnets in a self-contained cryostat.

Method of reacting magnet loads: Use of a bucking cylinder, wedging of the inner legs of the TF coils, or reacting the TF coils directly from the central solenoid.

Vacuum boundary: Use of a common boundary for the plasma and the magnets or the use of separate vacuum containment for each system

Number of replaceable modules: This varies from 12 to 48 depending upon the overall device configuration.



state current drive rely upon 400-500 keV neutral beams for central current drive and lower hybrid waves for current drive at the edge. The penetration of lower hybrid waves is felt to be inadequate for high density operation.

Table II.2.3-1  
Physics Constraints

	INTOR	NET	FER	TIBER	OTR
I(MA)	8	10.8	8.74	10	8
I	1.6	2.05	1.7	2.4	1.5
$\tau_E$ req.(sec)	1.4	1.9	1.7	0.44	1.7
$\tau_E$ (ASDEX-H) $\tau_E$ ,required	2.9	3.0	2.3	6.8	3
$n(10^{20}/m^3)$	1.6	1.7	1.14	1.06	1.7
Murakami( $10^{19}/T.m^2$ )	19	23	15	8	25
parameter*					
Beta Required (%)	4.9	5.6	5.3	6	3.2
Troyon Coefficient (%)	4	3.5	3.5	2.8	3.5
Impurity Control divertor	SN	DN	SN	DN	SN
Pulse length (sec)	150	350	800	55	600
Heating	ICRF	TBD	ICRF (LH ramp-up)	LH + NBI	ICRH

\*Computed using line average density

Component replaceability: Most designs assume many of the components to be designed to last the life of the device with no plan for replaceability; other designs make no such assumption.

Tritium breeding: This varies from no tritium breeding (other than in test modules) to full tritium self-sufficiency.

Maintenance approach: Two major approaches are considered; these are horizontal removal of torus components, or vertical removal of torus components.

Plasma configuration: The plasma configurations vary from modestly elongated (1.5) single-null divertor plasmas to highly elongated (2.4) double-null divertor plasmas.

Radial dimensions: The five designs vary dramatically in the overall plasma major radius, and naturally in the thickness of the components and space allocations comprising the major radius. For example, the allowance for plasma scrape-off varies from 9 to 30 cm, the total inboard blanket/shield thickness varies from 48 to 105 cm, the accumulated allowance for assembly gaps and spaces varies from 2 to 20 cm, and the thickness of the TF coil inner leg varies from 49 cm to 110 cm.

In the area of electromagnetics and heating and current drive technology, the major differences are in the electromagnetics. All of the designs are using similar heating and current drive technologies.

In the TF coil system, there are a number of different engineering design constraints being used. These are primarily related to the environment perceived necessary for the desired performance from the superconductor. These include the total and peak nuclear heating levels. The total nuclear heating level varies from about 8 to 72 kW of nuclear heat deposition; the related peak nuclear heating levels vary from about 0.3 to 5 kW/m<sup>3</sup>. Radiation protection requirements for the superconductor and the associated insulator also vary significantly; the radiation dose varies from about  $2 \times 10^8$  to  $10^{10}$  rads. Other significant variables are the conductor current values (from 16 to 35 kA), the average winding pack current density (from about 10 to 22 MA/m<sup>2</sup>), the magnetic energy (from 4 to 45 GJ), and the maximum quench voltage to ground (from about 7 to 20 kV).

In the PF coil system, the dominant differences are related to the total volt-seconds the system must provide (from about 50 to 210 V-s). In addition, there are differences in the allowable maximum field rate of change, varying from about 0.5 to 3 T/s; differences in the OH current ramp time, from about 13 to 30 s; differences in the breakdown voltage being used, from 10 to 35 s; and finally, differences in the total magnetic stored energy, from about 4 to 11 GJ.

In the nuclear systems area, there are significant differences in the engineering design constraints in a number of aspects of the first wall and blanket, the diverotr, and in the shield area.

In the first wall and blanket systems, these differences are related to the target lifetime fluence values (which range from 0.3 to 3 MWa/m<sup>2</sup>), the allowable stresses in the structural material which are also tied to the number of lifetime cycles of operation, the tritium breeding requirement, the first wall protection assumptions, and finally the assumptions related to the disruption scenario.

In the divertor area, the differences are related to the incorporation of different concepts for the physics and technology phases, and to the differences in the disruption scenario.

In the shield area, the differences are related largely to the need to protect the magnets so are tied to the allowable fluence to the superconductor, to the allowable dose to the insulators, and to the nuclear heating limits. A second constraint relates to the desire to minimize the overall thickness of the inboard shield region so as to minimize the size and cost of the design.

#### 2.4 Design Driving Features

The five INTOR-like designs differ in a number of significant features which tend to "drive" the characteristics of each design. Each of these design driving features represents an aspect of the design where the designer has a choice from among a number of options. These choices are made so as to be compatible with the overall mission and supporting programmatic and technical objectives established for each design.

The selection of each of the design driving features by each design team is also influenced by the judgement concerning a number of important considerations related to each national program. These include the perceived timing for the necessary development and construction of each device, the perceived understanding of the present scientific and technological data base and what advances can be made in the time period until the start of construction, and finally the maturity of the technology need to support each design and its stated mission.

Table II.2.4.1 presents a comparison of the major design driving features for the five INTOR-like designs. Many of these features are related to the scientific desires and present understanding. These include the need to achieve ignition or not, the nature of the operating scenario (inductive or non-inductive current drive, or some hybrid combination), the pulse length, the degree of plasma shaping (elongation), the type of impurity control (single or double null divertor), the nature of startup, and the plasma heating method. The remaining major driving features result from operational and technological considerations such as whether to breed tritium or not (and how much), the fluence target and the nature of the desired nuclear testing, and finally the approach to maintenance of the internal torus components (horizontal or vertical access).

Table II.2.4.1 Major Features of INTOR-like Designs

Feature/Parameter	INTOR	NET	FER	TIBER	OTR
Major radius (m)	5.00	5.18	4.42	3.00	6.30
Minor radius (m)	1.20	1.35	1.25	0.83	1.50
Ignited or Q	Ignited	Ignited	Q > 20-30	Q > 5	Q > 5
Pulse length (s)	150.00	>200	800.00	CW	600.00
Impurity control	SN	DN/SN	SN	DN	SN
Operating scenario	Induct.	Induct.	Hybrid	Noninduct.	Induct.
Elongation	1.60	2.20/1.60	1.70	2.40	1.50
Triangularity	0.25	0.70/0.30	0.20	0.40	0.30
Fluence objective, MWy/m <sup>2</sup>	3.00	0.80	0.30	3.00	5.00
Tritium breeding	>0.60	>0.3	None	>1.0	>1.05
Plasma heating method	ICRH	(TBS)	(TBS)	NBI + LH	ICRH
Access for maintenance	Horizontal	Vertical	Horizontal	Horizontal	Horizontal



## 2.5 Systems Analysis

A systems analysis of the five INTOR-like designs (FER, NET, TIBER, OTR, and INTOR) was performed. This study was established to evaluate and quantitatively determine the reasons for differences between the five designs and to determine the specific impact produced in a given design by making a specific change in that design. This quantitative analysis provides valuable insight on how different choices affect a given design. The results should be valuable in the development of the next generation of tokamak designs.

### Systems Analysis Code - TETRA

Systems Analysis methodology has progressed significantly during the last several years. The capability has been developed to represent a tokamak point design and much of the complexity of the various systems comprising the design as well as their multiple interactions. Numerical optimization methods have been incorporated that enable simultaneous change of many variables subject to specified constraints. These many features are incorporated into the Tokamak Engineering Test Reactor Analysis (TETRA) systems code developed under the leadership of the Fusion Engineering Design Center (FEDC).

### Replication of INTOR-like Designs

A significant test of the systems analysis methodology is the ability to replicate various tokamak designs. A measure of the validity, and usefulness, of the methodology is the ability to reproduce the major features and performance of a variety of designs. One test of this ability is to use the systems analysis method to reproduce as accurately as possible (i.e., to replicate) the mechanical features, performance, physics parameters, and engineering parameters of an existing tokamak design. The systems analysis process requires some input to be provided. With this

input, certain output is generated. The TETRA systems code was used to replicate each of the five INTOR-like designs.

The results of these calculations demonstrate a good ability to accurately represent the general, as well as many specific features and parameters of the designs. This demonstrated good ability provides confidence that parametric studies should provide meaningful indications of the impact of making a given change to a design.

#### Sensitivity Analysis

Sensitivity calculations were performed relative to the TIBER design to determine what changes are produced by making deliberate changes in selected input. Calculations were performed in which one aspect of the design was changed (such as a mechanical feature or dimension, a physics assumption or parameter, or an engineering assumption or parameter). The impact on the design resulting from this single change was determined.

The results of this set of calculations to investigate design sensitivity to changes in individual items allow an assessment of which items have a high leverage impact on the overall design and which items have considerably less impact. By performing a systematic assessment of which items have what impact on the design, the highest leverage items can be identified. Once identified, this information can be factored into the detailed design process and thereby provide guidance to the designers who have to develop the design in detail.

From the calculations, the results indicate that the items, or parameters, that demonstrate the greatest sensitivity include:

Energy Multiplication Factor - Q

Safety Factor, q

Elongation

$Z_{eff}$

Neutron Wall Load

Beta g-coefficient (Troyon factor)

The items, or parameters, that demonstrate the least sensitivity include:

Shield Thickness

Scrape-off layer (inboard)

Plasma profiles

There is an important distinction between parameter sensitivity and design impact. To draw practical conclusions from the sensitivity results, it is necessary to fold into the assessment the likely range of variation, or uncertainty, of a given parameter to determine the importance of a change in that parameter to the design. Parameters that have the greatest sensitivity will also have a large impact on the design even if the range of variation of that parameter is large or not. However, parameters that have the least sensitivity could still have a large impact on the design if the range of variation, or uncertainty, in that parameter is large. This practical consideration should be recognized in the design process.

Calculations were also performed in which a collection of items was changed. For example, it was of interest to determine the effect of substituting, at one time, all physics-related assumptions made in one design into a second design. It was also of interest to examine the effect of making similar collective changes of the engineering assumptions, or in the definition of the general features of the design.

Differences in the individual assumptions of the INTOR-like designs can be collectively grouped together into categories such as "physics," "engineering," or "features." The "physics" category typically includes terms such as beta and beta coefficient, safety factor, ignition margin, plasma temperature

and density, edge ripple, plasma profile factors, etc. The "engineering" category typically includes dimensions of components (ohmic heating (OH) and toroidal field (TF) coils, bucking cylinder, shield, etc.), stress levels, radiation dose levels, gaps, etc. The "features" category typically includes plasma configuration (elongation and triangularity), maintenance approach, fluence level, tritium breeding, single-null or double-null divertor, operating scenario, etc.

These studies were performed in general in a manner similar to the individual sensitivity studies just described. For example, studies were performed in which a calculational transition was made from the INTOR design to the TIBER design and from the NET design to the TIBER design.

The results from these studies indicate that the transition from one design to another can be made. This successfully demonstrates the ability to substitute global groupings of changes (all "physics," "engineering," or "features") and make the transition from one design to another.

In all of the systems analyses calculations, no single figure-of-merit seems to exist that should be used to best measure the impact of sensitivity calculations. Valuable measures include major radius and cost. However, for a given design, the impact of changes must still be interpreted with caution since the changes may also imply impacts on less measurable design aspects such as:

- o altering the risk associated with the design,
- o implying new technology developments or new physics,
- o implying maturity of technology changes, or
- o implying different timing relative to construction.

#### Relative Cost Estimates

There is an ongoing, and important, interest in how the estimated capital cost is impacted by various aspects of a tokamak



design. It is recognized that in any international comparison study, the various national designs are costed by each country using the national procedure to account for engineering fabrication, transportation, installation, and project management costs. These national approaches are all different, not only in the units of currency used, but in how the various cost elements are treated in the costing process. Recognizing these differences, a cost comparison was performed by the US for each of the five INTOR-like designs to determine the relative ranking of capital cost and to later compare with similar information generated by the other INTOR participants.

The relative capital costs were normalized to the INTOR cost estimate. The results indicate the following:

1. The costs for INTOR and NET are approximately the same,
2. The costs for FER are about 10% less than the cost of INTOR,
3. The costs for TIBER are about 35% less than the cost of INTOR, and
4. The costs for OTR are approximately 40% greater than the costs of INTOR.

These relative cost comparisons must be interpreted with care since the various designs make different assumptions about the timing of construction, the amount of supporting development and research required, and the aggressive or conservative posture regarding the maturity of the technology in the design. Factoring these considerations into the design can alter these cost comparisons, perhaps dramatically.

### Conclusions

Overall, this comparative systems analyses has demonstrated that valuable insights can be derived from such analyses. An important consideration is that these studies can be performed rapidly, at little cost. The results can provide valuable

guidance to the evolution of any given design. In this sense, such analyses are of high interest and value at the early stages of the design to provide rapid evaluation of many options. Generation of such a design data base of information at the early stages of the design establishes a strong quantitative support base for initial choices among options. Such choices permit the design team to focus quickly and engage in more detailed design efforts based on a reasonably established initial baseline design.

### 3. IMPLICATIONS FOR THE INTOR DESIGN CONCEPT

The principal conclusions from the work of Phase Two A, Part 3, and their implication for the INTOR design are summarized in the following sections.

#### 3.1 Impurity Control

Modelling studies and experimental data still support the choice of the poloidal divertor for impurity control and the choice of a high-z (tungsten) divertor collector plate surface. Thus, the major aspects of the recommended impurity control system are the same as in the reference INTOR design concept. A number of modifications to the INTOR design concept may be necessary, however. A low-z limiter for startup may be required. If the present uncertainty regarding severity of disruptions remains, then it may be prudent to install protective armour on the first wall, at least during the initial phase. The value of  $Z_{\text{eff}}$  may have to be increased from 1.5 to 2.0, in which case allowance would have to be made for a corresponding increase in the power radiated to the first wall.

#### 3.2 Operational Limits and Confinement

A variety of H-mode energy confinement scaling laws have been proposed over the last years. On the basis of these laws, the INTOR design concept is considered to have adequate confinement capability to achieve ignition, if there is no substantial degradation with heating power.

The INTOR design concept somewhat exceeds both the Murakami-Hugill limit and the Greenwald density limit, but it should be noted that these limits are

exceeded by as much as a factor of two in experiments with intense auxiliary heating. Thus, the density in INTOR is very probably below the actual density limit.

Analytical and experimental results indicate that the Troyon beta limit g-factor must be reduced from the value of 4 used in the INTOR design concept to 3.0 - 3.5 and that the safety factor  $q_I$  must be increased from 1.8 to at least 2. Since

$$\beta (\%) = \frac{g I_p (\text{MA})}{a (\text{m}) B (\text{T})}$$

$$q_I = \frac{5 \left[ \frac{1}{2} - \left( 1 + \left( \frac{b}{a} \right)^2 \right)^{1/2} \right] B (\text{T}) a^2 (\text{m})}{R (\text{m}) I_p (\text{MA})}$$

a combination of increasing the plasma current, the magnetic field and the plasma elongation (b/a) and/or reducing the major radius in the INTOR design concept is probably necessary to achieve the performance objective (e.g. neutron wall load).

### 3.3 Current Drive and Heating

There is now a substantial experimental and theoretical database on non-inductive current drive, for example by lower hybrid waves or neutral beams or a combination of both so that it can be considered as an option to achieve the performance objectives of INTOR. However, the predicted efficiency is low,

and the required power may be of the order of 100 MW if the plasma parameters are optimized for current drive. Thus, while inductive current drive is retained as the reference option in the present INTOR design concept, it is suggested to use noninductive current drive in a new INTOR-like design concept, provided that such a design could be shown to be feasible and to have substantial advantage over an inductively driven design.

New experimental data support the previous choice of ICRH as the reference heating scheme in INTOR. However, if neutral beams and lower hybrid waves were chosen for current drive in a new INTOR-like design concept, it would be appropriate to use them also for heating (and in case of neutral beams for added impurity control by flow reversal).

### 3.4 Electromagnetic

It has been established that the active control coils should be located inside the toroidal field coils and outside the shield. Also, it has been confirmed that the first wall/blanket structure is adequate for passive stabilization.

Modelling studies indicate that the INTOR poloidal field coil system could be designed more optimally. In particular, the coils should be placed closer to the midplane. leaving a large midplane window for horizontal access imposes a moderate penalty in terms of stored energy for little elongated to moderately elongated plasmas, but a large penalty for highly elongated plasmas.

### 3.5 Configuration and Maintenance

The reference INTOR maintenance concept is horizontal removal of large torus



segments, which requires that a rather large 'window' for access be left at the midplane, with the consequence that no poloidal field coils can be located near the midplane. Analysis of this maintenance scheme and comparison with a vertical or oblique removal concept led to the conclusion that the simpler maintenance procedures associated with horizontal maintenance outweigh the penalty in poloidal field coil optimization for small to moderate plasma elongation, but that the vertical or oblique maintenance scheme is preferable for moderate to large plasma elongation, for which the penalty in poloidal field coil optimization becomes too large. Thus, if the plasma elongation has to be increased to more than two, as may be necessary to satisfy the plasma operating limits, (see vertical or oblique concept may be required. Section 2.4.2), then change from the horizontal maintenance concept to the vertical or oblique concept may be required. Also a combination of the two concepts might have its merits.

For the reference INTOR maintenance concept, it is recommended to use a transfer cask for containing tritium and dust, in order to meet the requirement of personnel access to the reactor hall. Because of recent developments, an in situ maintenance scheme is recommended for components facing the plasma (e.g. protective tiles on the first wall).

The use of iron inserts to reduce the field ripple would enable a reduction of about 50 cm in the toroidal field coil bore or a reduction in the number of coils from twelve to ten, without significantly complicating the configuration. Thus, the use of iron inserts is recommended.

### 3.6 First Wall and Blanket

Analyses of the divertor collector plate, the first wall and the breeding blanket confirm the choices that were made in the INTOR design concept. The

reference divertor plate concept of tungsten tiles bonded to a water cooled copper heat sink is predicted to have a lifetime of  $2 \times 10^4$  cycles, limited during normal burn by fatigue and erosion. This implies that the divertor plate must be replaced ten times during the lifetime of INTOR. It is still recommended to use a bare, water-cooled austenitic stainless steel first wall, unless new information indicates that the frequency of disruptions would be much greater than is assumed in the present disruption scenario.

The reference breeding blanket concept, with ceramic breeding material, an austenitic stainless steel structure and water cooling, is still recommended. It is possible to use water at relatively low pressure, which is recommended for better reliability.

In the studies it was found that a beryllium multiplier together with certain design stratagems can be used to achieve a tritium breeding ratio greater than unity and hence to make INTOR self-sufficient in tritium production without increassing the inboard dimension or the level of risk. Accordingly, it is recommended to equip INTOR with a non reactor-relevant, tritium producing blanket adequate to provide tritium self-sufficiency.

### 3.7 Design Sensitivity

Systems analyses indicate that the size and cost of an INTOR-like design is very sensitive to the ignition margin,  $Z_{eff}$ , the plasma elongation, the safety factor, the value of the g-factor in the Troyon beta limit, the neutron wall load, the shield attenuation and the allowable stress in the toroidal field coils. Thus, the size and cost of INTOR could be reduced by future developments

that would lead to improved energy confinement, improved impurity control, stability at larger plasma elongation, lower safety factor, larger values of the Troyon g-factor, a higher limit of radiation damage on the magnet insulators, and magnet structural materials operating at higher stress levels.

## References

1. M. Ono, in Applications of Radio-frequency Power to Plasma, S. Bernabei and R. W. Motley, eds. American Institute of Physics, New York (1987), p. 230; M. Ono et al., Phys. Rev. Lett. 60(1988)294.
2. R. J. Hawryluk et al., in Plasma Physics and Controlled Nucl. Fusion Research 1986, IAEA, Vienna (1987), v.i., p. 51.
3. T. Nagashima et al., in Applications of Radio-frequency Power to Plasma, op cit., p. 94.
4. D. A. Ehst et al., Nucl. Eng. and Design/Fusion 2(1985)305; D. A. Ehst et al., Nucl. Eng. and Design/Fusion 2(1985)319; D. A. Ehst et al., Nucl. Eng. and Design/Fusion 3(1985)113.
5. C. F. F. Karney and N. J. Fisch, Phys. Fluids 29(1986)180.
6. IAEA INTOR-related Specialists' Meeting on Noninductive Current Drive; available from Max Planck Inst. of Plasma Physics (Garching) as report NET-PM-86-003; also as report IAEA-TECDOC-441, IAEA (Vienna) 1987.
7. D. A. Ehst and K. Evans, Jr., Nucl. Fusion 27(1987)1267.
8. F. X. Söldner, in Applications of Radio-frequency Power to Plasmas, op cit., p. 102.